UC San Diego
UC San Diego Previously Published Works

Title

Performance of a transparent Flexible Shear Beam container for geotechnical centrifuge modeling of dynamic problems

Permalink

https://escholarship.org/uc/item/76v7j40g

Authors

Ghayoomi, Majid
Dashti, Shideh
McCartney, John S

Publication Date

2013-10-01

DOI

10.1016/j.soildyn.2013.07.007

Peer reviewed

Performance of a Transparent Flexible Shear Beam Container for Geotechnical Centrifuge Modeling of Dynamic Problems

Majid Ghayoomi, Ph.D., Corresponding Author
Department of Civil Engineering
University of New Hampshire
W175 Kingsbury Hall
33 Academic Way
Durham, NH 03824
Phone: (603) 862 3997
Email: majid.ghayoomi@unh.edu

Shideh Dashti, Ph.D. and John S. McCartney, Ph.D., P.E.
Department of Civil, Environmental and Architectural Engineering
University of Colorado Boulder, UCB 428, Boulder, CO 80309

7/22/2021

ABSTRACT

A transparent Flexible Shear Beam (FSB) container was designed and constructed to simulate the dynamic response of a stratum of soil under horizontal, one-dimensional (1-D) earthquake shaking in a geotechnical centrifuge. A stack of four rectangular, acrylic frames separated by layers of flexible, high-strength rubber was used to form the transparent container. The fundamental natural frequency of the container was estimated to be similar to a layer of sand in its softened or liquefied state. The suitability of the container in simulating 1-D site response with minimal boundary effects was evaluated by monitoring the uniformity of the induced accelerations and settlements across the soil specimen. Further, the measured lateral displacements were compared with equivalent-linear site response analyses. The new FSB container was found to provide satisfactory boundary conditions for studying complex soil-structure-interaction problems, while simultaneously enabling researchers to visualize deformations of the soil and buried structures during shaking.

KEYWORDS: Flexible Shear Beam Container, Centrifuge Modeling, Physical Modeling, Boundary Effects, Seismic Soil-Structure-Interaction.

1. INTRODUCTION

Centrifuge modeling is commonly used in geotechnical engineering to simulate the response of a semi-infinite soil medium within the constraints of a small-scale, finite domain. The self-weight body stresses encountered in a prototype soil layer are replicated realistically in the centrifuge model, which permits other engineering parameters to be scaled using the concept of geometric similitude [1]. A 1:1 scale factor for stress enables researchers to capture the nonlinear, stress-dependent soil properties in centrifuge tests. In addition, physical modeling of the seismic response of a soil-structure system in a geotechnical centrifuge is advantageous because large scale, prototype tests are time consuming and expensive. The selection of an appropriate container that can properly simulate free-field boundary conditions and a one-dimensional (1-D) soil response under horizontal shaking is a challenge in geotechnical centrifuge modeling of dynamic problems. An ideal container in this case is expected to: (1) maintain a horizontal cross-section; (2) ensure that dynamic shear stresses developed on the soil-container interface are equal to those on horizontal planes; (3) have a negligible mass; (4) provide no additional lateral stiffness to the soil layer; and (5) provide no resistance against soil settlement [2,3].

Different types of model containers have been designed to capture the response of soil during 1-D shaking while minimizing boundary effects. Among the criteria mentioned above, the lateral stiffness of the container boundaries is the main variable that controls its dynamic response and the boundary effects. Hence, several types of containers varying in stiffness have been developed in response to different research applications and priorities, each with unique dynamic properties and associated boundary conditions. The stacked-ring apparatus [2;3], the laminar container [4,5], the Equivalent Shear Beam (ESB) container [6], the Flexible Shear Beam (FSB) container [7], and the hinged-plate container [8] are a few examples of centrifuge containers with different dynamic properties and

2

applications. Transparent, rigid containers are also commonly used to monitor the dynamic response of buried structures or track the movement of soil particles during shaking [9]. However, rigid containers are unable to produce realistic boundary conditions for dynamic problems, which may lead to unrealistic experimental results. Hence, using a transparent, rigid container typically implies that the researcher has prioritized visualization over realistic boundary conditions.

The ESB and FSB containers are commonly used to evaluate the dynamic response of soil and soil-structure systems during 1-D horizontal base shaking in centrifuge. The ESB container represents the initial lateral stiffness of a target soil specimen with a specific relative density (D_r) and height at the target level of spin acceleration [6]. Therefore, ESB-type containers do not capture the softened soil response at higher levels of induced strain and acceleration. An FSB container is a special case of ESB, with a lateral stiffness that is representative of a target soil layer in its softened state during dynamic loading. Although the very soft lateral stiffness (i.e., low fundamental natural frequency) of an FSB container is particularly advantageous when modeling a liquefiable soil deposit, it may also be used with a stiffer soil specimen, because it does not add to the lateral resistance of the system (e.g., criteria No. 4 above). Similar to the FSB container, laminar containers have a low lateral stiffness and have been widely used for simulating the response of different types of soil deposits successfully. However, the FSB container useful in simulating the dynamic response of complex soil-structure systems in a centrifuge, primarily because of its simple and continuous boundaries. In addition, special care is required to prevent water and soil particles from penetrating into the gaps between the frames in a laminar container, which is not necessary in an FSB container. All the available flexible containers are traditionally made of aluminum, preventing successful visualization of soil-structural movements from the sides during testing.

In this paper, the design and development of a new container are discussed. The container combines the advantages of an FSB container with those of a transparent rigid box. The dimensions and capacity

of the container were configured for the 1-D shaking table available at the geotechnical centrifuge facility at the University of Colorado Boulder (CU Boulder). The design of the container involved characterizing its fundamental frequency using a 3-D Finite Element model implemented in ABAQUS [10]. In addition to the ABAQUS analysis results, this paper presents the results of several shake table tests performed on the container at different gravitational accelerations to characterize its performance [11]. The 1-D, hydraulic, servo-controlled shake table mounted on the CU Boulder centrifuge was used in these experiments [12]. First, the dynamic response of the container was evaluated at different levels of spin acceleration, to validate the theoretically estimated performance variables. Then, boundary effects in the container were examined by evaluating the uniformity of accelerations within a sand specimen at different depths during a range of different, broadband ground motions. The measured accelerations and lateral displacements were compared with those estimated using 1-D, equivalent-linear, site response analyses implemented in DEEPSOIL [13]. Finally, the ability of the container to model seismic Soil-Structure-Interaction (SSI) locally with minimum boundary effects was evaluated by comparing near-field and free-field surface motions recorded under a range of input motions.

2. DESIGN, CONSTRUCTION, AND CHARACTERIZATION OF THE CONTAINER

A new transparent, Flexible Shear Beam-type (FSB) container was designed and constructed to model a 1-D, infinite half-space soil layer in the centrifuge. This container was designed to represent the lateral stiffness of a soil deposit in its softened state, with a low fundamental frequency. An FSB-type container was selected because it is expected to have a negligible influence on the effective lateral stiffness of the soil specimen due to its relatively soft response. A relatively simple container design with continuous and known boundaries is also advantageous in the physical modeling of complex soil-structure systems, particularly when the soil specimen is saturated.

The new FSB container, with inside dimensions W × L × H = 698 × 305 × 338 mm, was constructed of four, 71 mm-thick, rectangular, transparent, acrylic frames stacked on top of each other

4

and separated by sheets of 13 mm-thick Neoprene rubber. Transparent acrylic frames were used to permit visualization of the soil and buried structure response during and after earthquake loading. The rubber sheets were bonded to the acrylic frames using a high-strength, adhesive epoxy (Model 320/322 from Lord, Inc. of GIVE CITY and STATE). The epoxy also served as a hydraulic seal to prevent water leakage from saturated soil specimens. The stacked frames were connected to an anodized aluminum bottom plate to connect to the shake table. The bottom plate incorporates a recessed cavity, which can accommodate a drainage layer (i.e., gravel or geosynthetic) as well as drainage ports. The drainage ports facilitate both upward infiltration of water for saturation of soil, as well as drainage boundary conditions for evaluation of infiltration and drainage from partially saturated soil layers [14]. Similar design principles implemented by Zeng and Schofield [6] were employed in this container to satisfy the frictional conditions at the boundaries. A set of threaded shear rods were connected to the base plate in both ends of the container to sustain induced complimentary shear stresses under 1-D cyclic loading along the length of the container. The smooth, polished surfaces of the acrylic frames minimize the wall-soil friction in the direction of shaking, so that negligible shear stress is induced at the side boundaries. Additional aspects of the container design and component characteristics are described by Ghayoomi et al. [15]. A photograph of the assembled container with a dry sand layer mounted on the centrifuge shake table is shown in Figure 1(a), while a schematic of the container with relevant dimensions is shown in Figure 1(b).

Cast acrylic has a lower Young's modulus and moment of inertia compared to the hollow aluminum frames normally used in other FSB containers. Thus, bending and lateral deflection of the lower frames along their longer span due to large lateral earth pressures under increased gravity was a concern. The mid-point side-deflection of the frames was initially calculated using a simply supported beam theory [16], and the acrylic frames were designed to be thick enough to minimize lateral deflection. Further, the bottom frame was braced in the direction normal to the shake table motion

5

using an aluminum bracket, to reduce the likely deformations where maximum earth pressures are expected. After the container was fabricated, lateral deflections were measured along the length of the four frames under static conditions when filled with sand and spun to a centrifugal acceleration of 80 g, using horizontally-oriented LVDTs connected to an external rack. The largest measured lateral deflection was in the middle of the long side of the top acrylic frame (due to its one-sided constraint and no external bracing), which was less than approximately 0.5 mm in model scale under a centrifuge acceleration of 80 g. The lower frames deflected less than this amount as they were externally braced. The total soil surface settlement upon spin-up to 80 g was less than 0.2% of its initial height, which was partially due to frame deflections and partially due to densification under increased gravity. The small amount of settlement caused by frame widening is not expected to change the density of the soil, as the total volume and mass remains the same. And in general, the net change in sand relative density during spin-up falls within the range of uncertainty with the available pluviation methods. Hence, the small amount of frame deflection was judged to have a negligible impact on soil relative density and dynamic properties.

The thickness and modulus of the Neoprene rubber was selected so that the container would have the target values of flexibility and fundamental natural frequency. The details of the Neoprene rubber pads were reported in detail by Ghayoomi et al. [15]. Unconfined compression tests were initially performed on different types of rubberusing an MTS compression machine to characterize their pressure-dependent, elastic moduli [15]. The influences of rubber thickness and elasticity modulus on the dynamic stiffness of the container were subsequently evaluated through steady-state, frequency-domain, 3-D finite element analyses in ABAQUS. Based on the results of the analyses, a 13 mm-thick, soft high-strength rubber material was selected. The physical and mechanical properties of the Neoprene rubber implemented in the ABAQUS simulations are summarized in Table 1.

Due to the uncertainties in material properties, the numerically-predicted response of the container was validated experimentally after construction. The completed FSB container was mounted on the 1-D shake table inside the centrifuge. Horizontal accelerometers were mounted on each acrylic frame to measure the fundamental frequency of the container in the direction of the shake table motion. A series of sine-sweeps with a range of amplitudes were applied to the base of the container, and the top-to-base acceleration "Transfer Functions" were calculated. An input sine-sweep included a sequence of independent sinusoidal motions with the same amplitude but changing frequencies (e.g., model-scale frequencies ranging from 10 to 300 Hz), with 10 cycles at each frequency. The frequency response transfer function between two horizontal acceleration-time histories (denoted as x and y) may be calculated as the ratio of the amplitude of the two records in the frequency domain. The transfer function is commonly smoothed or calculated as the ratio of the corresponding power spectral density functions for an easier identification of dominant modes [17]:

$$T_{xy}(f) = \frac{S_{xy}(f)}{S_{xx}(f)} \tag{1}$$

where $S_{xx}(f)$ is the power spectral density function of motion x, and S_{xy} is the cross spectral density function of motions x and y. The transfer function representing the dynamic response of the container (i.e., top frame compared to the base) was obtained numerically (using ABAQUS) and experimentally (from accelerometer measurements), as shown in Figure 2. Reasonable agreement was observed between the two, and a fundamental natural frequency of approximately 38 Hz in the model scale was inferred for the completed, empty container at 60 g of spin acceleration (i.e., 0.63 Hz in the prototype scale). The natural frequency of the container is expected to vary at different centrifugal accelerations, due to the change in rubber stiffness at higher confining pressures. The natural frequency of the container at 1, 25, and 60 g was measured as 24, 36, and 40 Hz in the model scale (24, 1.44, and 0.67

Hz in the prototype scale), respectively [15]. This implies a softer prototype dynamic response for the container at higher g-levels, which is in line with the philosophy of using an FSB container.

3. EVALUATION OF CONTAINER BOUNDARY EFFECTS

3.1. Centrifuge Testing Program

A series of four dynamic centrifuge tests, summarized in Table 2, were performed on a representative free-field soil specimen and a soil-structure model to evaluate the performance of the FSB container in simulating 1-D site response and to characterize its boundary effects. The performance of the container was investigated under a range of model conditions and broadband input ground motions. Accelerometers were used to measure horizontal accelerations within the soil specimen, on an embedded structure, and on each container frame. Vertical displacements of the soil layer and structure as well as the horizontal displacement of each container frames were measured using LVDTs attached to external racks. The centrifuge test results presented in this paper are presented in prototype-scale engineering units unless indicated otherwise.

3.1.1 Soil Properties

In all tests, a 338 mm-thick (model scale) layer of #120 Nevada sand with a relative density (D_r) ≈ 60% was formed in the FSB container by dry pluviation using a barrel hopper. Nevada sand was used as it is a well-characterized, fine, uniform, and angular sand that is commercially available. The material properties of the batch of Nevada sand used in this study are summarized in Table 3 and its grain size distribution is shown in Figure 3.

3.1.2 Ground Motion Selection

The dynamic response of the soil specimen and model container was evaluated initially under the low-amplitude, ambient vibration of the centrifuge basket caused by air turbulence inside the centrifuge chamber. In addition, two earthquake motions were selected with consideration of their characteristics in terms of frequency content, duration, amplitude, Arias intensity [19], and rate of energy buildup. The

rate of energy buildup may be defined by the Shaking Intensity Rate (SIR) as the slope of the Arias

Intensity time history [20]. The Arias Intensity-time history is defined as:

$$I_a(t) = \frac{\pi}{2g} \int_0^t a^2(t)\, dt$$

(2)

where a(t) is the measured acceleration time history and g is the gravitational acceleration. The SIR is

defined as:

$$SIR = I_{a5-75}/D_{5-75}$$

(3)

where I_{a5-75} is the change in Arias intensity from 5 to 75% of its final value, and D_{5-75} is its

corresponding time duration.

The fault-parallel component of the 1999 Izmit (Kocaeli) Earthquake in Turkey recorded at the

Istanbul Station (IST180), which was scaled to a Peak Ground Acceleration (PGA) of 0.1g, represented

a less intense, far-field event with a long duration (see Table 4). The fault normal component of the

1992 Landers Earthquake recorded at the Joshua Tree Station (JOS090) applied at its original scale

(PGA = 0.3g) represented a moderate intensity and duration motion with the backward directivity

effect. These motions will be referred to as the Ambient, Izmit, and Landers motions, respectively.

The acceleration-time histories of both Izmit and Landers earthquake motions were passed through

an 8th order, acausal, low-pass, Butterworth filter with a corner frequency of 15 Hz. The goal was to

avoid frequencies beyond the shake table's controllable frequency range (i.e., approximately 10 to 300

Hz in the model scale). Since the frequency content of the motions were above the minimum limit, no

high-pass filter was applied. Lastly, these motions were base-line corrected and scaled based on the

centrifuge scaling laws. The command signal sent to the shaker was calibrated using a trial soil

specimen in the new container to achieve a reasonable match between the desired and achieved

motions in terms of spectral accelerations and Arias Intensity-time histories [21]. The acceleration

time-histories and the 5%-damped spectral accelerations of the achieved earthquake motions at the base

of the container (i.e., Izmit and Landers motions) are shown in Figure 4. In addition, the primary ground motion index properties are listed in Table 4.

3.2. Test Results

3.2.1 *Free-Field Soil Response under Ambient Condition*

The response of an 18.6 m-thick (prototype scale), free-field (i.e., with no structure), dry, medium dense sand deposit was initially investigated under ambient loading conditions at 55g of spin acceleration (i.e., Test FF-AMB55 in Table 2). The goal was to measure the initial natural frequency and dynamic properties (e.g., shear modulus) of the sand specimen at small strains, before major softening. Small-strain dynamic properties are critical in site response analyses, which were later conducted to evaluate the performance of the container in simulating 1-D site response. The instrumentation layout and model dimensions are shown in Figure 5. Two vertical arrays of accelerometers were placed in the free-field soil model. The central accelerometer array was placed in the middle of the container (both across the length and width), while the side array was placed 254 mm off-center along the length. The top-to-base transfer function of soil response during ambient loading was calculated based on the accelerometer measurements in the central array, as shown in Figure 6. A soil natural frequency of approximately 2.4 Hz was measured in this manner, which was then compared with analytical estimates, as follows:

The natural frequency of the soil deposit at a particular strain level depends on its shear modulus, which changes with depth. Idriss and Seed [22] proposed the following equation for the natural frequency of an inhomogeneous soil layer with shear modulus G defined as a function of depth (i.e., $G = Az^p$; $0 < p \leq 0.5$), based on the 1-D wave propagation solution:

$$f_n = \frac{\beta_n}{2\pi} \frac{2-p}{2} \frac{\sqrt{A/\rho}}{H^{\frac{2-p}{2}}} \tag{4}$$

where f_n is the nth natural frequency of the soil layer, p is the depth power in the shear modulus equation, A is a fitting parameter, ρ is the total density of the soil, and H is the soil height. Factor β_n represents the roots of the Bessel function, $J_{(p-1)/(2-p)}(\beta_n) = 0$. The shear modulus at small strains, G_{max}, may be used to estimate the soil specimen's initial fundamental frequency before softening (similar to what is expected under ambient loading). The small strain shear modulus can be defined using several different empirical relationships, such as the one defined by Seed and Idriss [23]:

$$G_{max} = 1000 * K * (\sigma'_m)^{1/2}$$

(5)

It can also be defined using the equation proposed by Hardin and Richart [24]:

$$G_{max} = 700 \frac{(2.17-e)^2}{1+e} * (\sigma'_m)^{1/2}$$

(6)

where K is a function of relative density, e is the void ratio, and σ'_m is the mean effective stress. The mean effective stress and shear modulus are in psf and ksc in Equations 5 and 6, respectively. A value of K of 52 was estimated for Nevada sand with D_r of 60% (e = 0.69), while σ'_m was estimated as a function of depth (z) for sand using a dry density (ρ_d) $\approx$ 1565.8 kg/m³ (e.g., Table 2). The equivalent depth-dependent, small-strain shear modulus were estimated to be $G_{max} = 3.6 \times 10^7 (z)^{1/2}$ and $G_{max} = 2.8 \times 10^7 (z)^{1/2}$ using Equations 5 and 6, respectively. Accordingly, the initial, first mode natural frequency of an 18.6 m-thick, dry sand deposit with $D_r \approx$ 60% was calculated using Equation 4 to be 3.4 to 3.8 Hz (shown in Figure 6).

The initial natural frequency of the sand specimen estimated analytically (e.g., 3.3 to 3.8 Hz) was greater than the measured value during the ambient test (e.g., 2.4 Hz). This difference may be partially due to the type of sand used in this study, which differs from those used to develop the empirical equations for G_{max} (Equations 5 and 6). Additionally, Equations 5 and 6 were proposed for shear strains in the order of 10^{-4}%, whereas additional shear strains might have been induced in the soil specimen even under ambient loading due to the vibration of the centrifuge bucket. Miniature accelerometers,

11

LVDTs, and bender elements are typically used in centrifuge model tests to measure strains in the soil. However, these instruments do not accurately measure such small values of shear strains during ambient loading due to the very low signal to noise ratio. This limited the ability to compare the strain levels from the two methods (i.e., experimental and empirical). The G_{max} value was back calculated from the measured fundamental frequency of $f_n \approx 2.4$ Hz using Equation 4. This G_{max} profile was approximately 52% of the analytical profile calculated from Equation 6 [24]. The G_{max} profiles with depth from both methods were subsequently used in the 1-D, equivalent-linear, site response analyses described in the next section.

One of the key characteristics of an ideal model container is having a softer lateral response compared the soil specimen. The measured soil natural frequency in the ambient test showed a much stiffer lateral response ($f_n \approx 2.4$ Hz) compared to the empty container ($f_n \approx 38$ Hz in the model scale, corresponding to $f_n \approx 0.69$ Hz in prototype scale when spinning to 55g). Thus, as intended, the container boundaries were laterally softer than the model soil layer (before softening) used in this study. Since the FSB container is intended to be used for simulating the response of soil specimens with different dynamic properties and stiffness, it was important to evaluate its response in relation to the stiffness of sand under both dry and saturated conditions under higher strain levels associated with earthquake loading. Elgamal et al. [25] showed experimentally that the shear modulus reduction curves for sand reach a residual value at large shear strains, and the shear modulus at large strains is within 20% of the corresponding values at small strains. This observation was applicable to both dry and saturated sand specimens under dynamic loading.

After applying an 80% reduction to the experimentally determined G_{max} profile in the sand specimen (i.e., ambient conditions), a natural frequency of approximately 1.1 Hz was estimated (using Equation 4) for an 18.6-m thick sand layer in its softened state. This value is well above the natural frequency of the empty container ($f_n \approx 0.7$ Hz in the prototype scale when spinning at 55g). In

12

addition, the performance of the FSB container with a softened soil layer (saturated sand) was evaluated in a separate set of tests at 77 g. A $f_n \approx 0.6$ Hz was measured in the sand deposit during dynamic loading that caused excess pore pressure generation and liquefaction (e.g., excess pore pressure ratio, $r_u \approx 1$) at some depths. This frequency was similar to and slightly greater than the estimated natural frequency of the container (i.e., ~0.5 Hz when spinning at 77 g). As a result, the container was judged to be soft enough not to affect the lateral response of sand even in its softened (liquefied) state.

3.2.2. Free Field Soil Response under Earthquake Loading

Simulating a 1-D soil response under vertically propagating, horizontal shear waves with uniform movements across the container at each depth is a key property of an ideal container. Further, an ideal free-field soil model represents an infinite half space, where the surficial response is the same across the cross section area of the container. The motion uniformity was checked by comparing the accelerations at several points at different soil depths across the container in test FF-IZM60. The response of a 20.3 m-thick, free-field sand deposit with $D_r \approx 60\%$ was simulated during the Izmit motion at 60g spin acceleration. The instrumentation layout and model dimensions are shown in Figure 5. Three sets of acceleration-time histories at equivalent prototype-scale depths of 2.1, 7.2, and 12.2 m were selected, and their corresponding Arias intensity (I_a) time histories and 5%-damped spectral accelerations are shown in Figure 7. These sets include data from two accelerometers inside the soil (one at the center and one off center) and one accelerometer on each container frame. The acceleration comparisons in the soil layer showed reasonable agreement, as the maximum difference between the recorded Arias Intensities across the container at a given depth did not exceed 5%. Similarly, the difference between spectral accelerations was less than approximately 5% across the container, with the exception of higher amplitude accelerations at lower periods (T $\approx$ 0.15 s to 0.35 s). The relatively small error in acceleration measurements indicates a satisfactory container performance in simulating an

approximately uniform 1-D soil response. The slight acceleration difference between the soil and container, which is minimal in lower frames, is due to the step-wise response of the container as opposed to continuous soil movement.

Soil surface settlement is another critical free-field measurement, the uniformity of which was checked during this experiment using LVDTs as shown in Figure 8. Two vertical LVDTs were installed across the container to measure soil surface settlements and monitor the change in soil relative density during each shake at the locations shown in Figure 5. The surface settlements measured at the two different locations shown in Figure 8 agree well.

Lastly, site response recorded during free-field experiments FF-LND77 was compared against 1-D, equivalent-linear site response analyses using DEEPSOIL V5.0. Of particular interest was the comparison between the measured lateral displacement profiles of the container with theoretical estimates assuming 1-D shaking of a free-field model. Five horizontal LVDTs were mounted on a vertical rack to measure the container's lateral displacement during each shaking scenario (e.g., Figure 5). The corresponding analytical model evaluated in DEEPSOIL included 21 sub-layers, 1 m in thickness for the top 16 layers and 2 m in thickness for the bottom 5 layers. The simulation was performed using the sand physical properties summarized in Table 4. The shear modulus reduction and damping equations proposed by Darendeli et al. [26] were used in these analyses. Further, the shear strength of the soil was considered, in addition to stiffness and damping. The modulus reduction curves were modified slightly at larger strains, so that the achieved friction angles and shear strengths remained constant under higher values of shear strain [27, 28]. Further, the shear wave velocity profile of sand was estimated from the G_{max} profile obtained: 1) experimentally from back-calculating the measured natural frequency during ambient loading conditions and 2) empirically using Equation 6. The recorded (achieved) acceleration-time history at the base of the model container was used as the input "within" motion in the DEEPSOIL analyses.

A comparison of the measured and computed 5%-damped spectral accelerations at the soil surface during experiment FF-LND77 is shown in Figure 9. A comparison of the measured and computed peak lateral displacement profiles of the container frames during the Landers motion in FF-LND77 is shown in Figure 10. The displacements were calculated at smaller depth intervals in DEEPSOIL, while experimental measurements were obtained only at the center of each frame. Even though equivalent-linear site response analyses have limitations, particularly at more intense levels of shaking, these comparisons showed reasonable agreement. The G_{max} profile estimated using Equation 6 resulted in a lateral deformation profile that better matched the experimental measurements, particularly at shallower depths. However, the calculated spectral accelerations at the soil surface using both G_{max} estimation approaches are higher than the measured ones, due to the limitations of an equivalent linear approach in capturing soil nonlinearities at strong levels of shaking. Overall, these results confirmed that the new FSB container simulates a nearly 1-D site response. The observed difference between the results is likely due to uncertainties in the material dynamic properties used in analyses and slight boundary effects that are expected in any container.

3.2.3. Soil-Structure-Interaction under Earthquake Loading

Physical modeling of seismic Soil-Structure-Interaction (SSI) was of primary interest in the development of the new FSB container. To evaluate the performance of the container in modeling SSI locally with minimum boundary effects, a representative single-degree-of-freedom (SDOF) structural model was embedded in an infinite half-space soil layer and subjected to the Landers motion at 77g of spin acceleration in Test SSI-LND77. Local SSI effects are expected near the structure and a response similar to free-field is expected when sufficiently away from the structure. This model structure represented a 4-story building (12 m-high) placed on a 1 m-thick mat foundation with a 6 m × 6 m contact area. The embedment of the structural model was equal to the thickness of the foundation (i.e., 1 m). The mass and columns of the structural model were made of steel and the foundation was made

15

of aluminum with a base contact pressure of 162 kPa. The fixed-base natural frequency of the structure was measured as approximately 4 Hz (i.e., equivalent to 310 Hz in model scale), representing a building with a first mode period of 0.25 s. The instrumentation layout and model dimensions in test SSI-LND77 are shown in Figure 11. Soil surface settlements were measured at two points using vertical LVDTs: LVDT7 placed 7.8 m away from the edge of the foundation (i.e., "near-field"); and LVDT8 placed 15.7 m away from the edge of the foundation (i.e., "far-field"). In addition, structural settlements were monitored using four vertical LVDTs placed at each corner of the mass.

Ideally, the structure must be far enough from the boundaries to produce localized SSI effects [6]. Under this condition, the near-field soil response is expected to be affected by the presence of a superstructure, while the response in the far-field would be similar to that of a free-field soil model. Thus, the container boundary effects on the soil system with and without the presence of a super structure were compared. The recorded accelerations in the free-field (e.g., Test FF-LND77) were compared with the corresponding far-field measurements in Test SSI-LND77, both subjected to the Landers motion. The corresponding comparison of Arias Intensity time histories and 5%-damped spectral accelerations on the soil surface are shown in Figure 12. The results show reasonable agreement between the far-field and free-field surface accelerations. The slight differences particularly manifested in the Arias intensities are attributed to the slightly different achieved input motions during the two sets of tests. The achieved input (base) motions in Tests FF-LND77 and SSI-LND77 are also compared in Figure 12. Further, soil surface settlements were compared for three conditions as shown in Figure 13: (1) free-field in test FF-LND77; (2) far-field in test SSI-LND77; and (3) near-field in test SSI-LND77. Similar settlements were measured in the free-field and far-field as expected, while higher settlements were observed in the near-field condition, indicating a localized SSI response and satisfactory container boundary effects.

4. CAPABILITY TO VISUALIZE THE RESPONSE OF UNDERGROUND STRUCTURES

A primary advantage of the newly constructed FSB container described in this paper is its ability to visualize the response of underground structures and displacement patterns in the centrifuge, while maintaining minimum boundary effects. The transparent FSB container may be used to investigate: soil particle movements inside a dry soil model; localized liquefaction-induced deformations near buildings or lifelines; seismic response of underground structures in a variety of soils; response of complex soil-structure-underground structure systems and their interactions. As an example, a photo of an ongoing experiment investigating soil-structure-underground structure-interaction in the transparent FSB container is shown in Figure 13, where a shallow underground structure is placed adjacent to a building, and the system is subject to a series of earthquake motions in flight. Racking (i.e., horizontal, shear type displacements across the cross section of the tunnel) is a key factor in evaluating the performance of shallow, rectangular box structures, which is typically difficult to measure accurately inside small structures on the centrifuge. The transparent container enables visualization of the response of the underground box structure using a high-speed camera. Racking deformations can be characterized using image analysis in this case.

6. CONCLUSIONS

A transparent Flexible Shear Beam (FSB) container was designed, constructed, and tested to ensure its satisfactory performance in modeling a stratum of soil under 1-D, horizontal earthquake loading with minimum boundary effects. The low natural frequency of the container (soft lateral response) is advantageous in modeling soil layers with a wide range of dynamic lateral stiffness. The fundamental natural frequency of the empty container at 60 g of spin acceleration was determined both numerically and experimentally, and was found to be approximately 38 Hz. Subsequently, a series of dynamic centrifuge experiments were performed on the container filled with dry sand, with and without a structure, undergoing a range of dynamic loading conditions. Accelerations measured in the free-field soil model across the container at different depths were primarily uniform, with a maximum difference

of approximately 5% in Arias Intensity-time histories and spectral accelerations. Similarly, soil surface settlements were generally uniform across the container. The close agreement between the measured free-field soil response and 1-D, equivalent-linear, site response analyses in terms of spectral accelerations and lateral displacements confirmed the ability of the container to simulate 1-D soil response under vertically propagating horizontal shear waves. The container's performance in the simulation of localized seismic SSI with minor boundary effects was evaluated in a centrifuge test, where a single-degree-of-freedom structural model with shallow foundation was placed on dry sand. Far-field soil response compared well with the free-field soil response under the same input motion. The close agreement between the free-field and far-field motions indicated a localized SSI effects. The newly constructed, transparent FSB container, with its relatively simple boundaries and minimized adverse boundary effects, is attractive for simulating the seismic response of complex soil-structure systems, while simultaneously enabling better visualization of the response of underground structures and soil particle movements.

ACKNOWLEDGEMENT

REFERENCES

[1] Garnier, J., Gaudin, S.M., Springman, S.M., Culligan, P.J., Goodings, D., Konig, D., Kutter, B., Phillips, R., Randolph, M.F., and Thorel, L., Catalogue of Scaling Laws and Similitude Questions in Geotechnical Centrifuge Modeling, International Journal of Physical Modelling in Geotechnics,

2007, 3, 1-23.

[2] Whitman, R.V., Lambe, P.C., and Kutter, B.L., Initial Results from a Stacked ring Apparatus for Simulation of a Soil Profile, Proceedings of the International Conference on Recent Advance in Geotechnical Earthquake Engineering and Soil Dynamics, UMR-Rolla, MO, 1981, 1105-1110.

[3] Whitman, R.V., and Lambe, P.C., Effect of Boundary Conditions Upon Centrifuge Experiments Using Ground Motion Simulation, ASTM Geotechnical Testing Journal, 1986, 9(2), 61-71.

[4] Hushmand, B., Scott, R.F., and Crouse, C.B., Centrifuge Liquefaction Tests in a Laminar Box, Géotechnique, 1988, 38(2), 253-262.

[5] Law, H., Ko, H.-Y., Sture, S., and Pak, R., Development and Performance of a Laminar Container for Earthquake Liquefaction Studies, Proceedings of the International Conference Centrifuge, Boulder, CO, 1991, 369-376.

[6] Zeng, X. and Schofield, A.N., Design and Performance of an Equivalent-Shear-Beam Container for Earthquake Centrifuge Modelling, Géotechnique, 1996, 46(1), 83-102.

[7] Divis, C.J., Kutter, B.L., Idriss, I.M., Goto, Y., and Matsuda, T., Uniformity of Specimen and Response of Liquefiable Sand Model in Large Centrifuge Shaker, Proceedings of the Sixth Japan-US Workshop on Earthquake Resistant Design of Lifeline Facilities and Countermeasures Against Soil Liquefaction, 1996, 259-274.

[8] Fiegel, G.L., Hudson, M., Idriss, I.M., Kutter, B.L., and Zeng, X., Effect of Model Containers on Dynamic Soil Response, Proceedings of the International Centrifuge Conference, Singapore, 1994, 145-150.

[9] Kutter, B.L., Chou, J.-C., and Travasarou, T., Centrifuge Testing of the Seismic Performance of a Submerged Cut-and-Cover Tunnel in Liquefied Soil, Proceedings of Geotechnical Earthquake Engineering and Soil Dynamics IV congress, Geotechnical Special Publication 181, ASCE, 2008, 1-29.

[10] Abaqus V.6-11, Users' Manual, Simulia, 2011.

[11] Ko, H.-Y., The Colorado Centrifuge Facility, Centrifuge 88, Corte, Ed., Balkema, Rotterdam, 1988, 73-75.

[12] Ketchum, S.A., Development of an Earthquake Motion Simulator for Centrifuge Testing and the Dynamic Response of a Model Sand Embankment, PhD Dissertation, University of Colorado Boulder, Boulder, CO, 1989.

[13] Hashash, Y., Deepsoil V5.0, UIUC, Users' Manual, 2012.

[14] Ghayoomi, M., McCartney, J.S., and Ko, H.-Y., Centrifuge Test to Assess the Seismic Compression of Partially Saturated Sand Layers, ASTM, Geotechnical Testing Journal, 34(4), 2011, 1-11.

[15] Ghayoomi, M., Dashti, S., and McCartney, J.S., Design and Construction of A Transparent Flexible-Shear-Beam container for Dynamic geotechnical centrifuge Testing, Second International Conference on Performance-Based Design in Earthquake Geotechnical Engineering, Taormina, Italy, 2012.

[16] Timoshenko, S., History of Strength of Materials, McGraw Hill, New York, 1953.

[17] Kim, S. and Stewart, J.P., Kinematic Soil-Structure Interaction from Strong Motion Recordings, ASCE Journal of Geotechnical and Geoenvironmental Engineering, 129(4), 2003, 323-335.

[18] Bardet, J.P., Huang, Q., and Chi, S.W., Numerical Prediction for Model No 1, Proceedings of International Conference on the Verification of Numerical Procedures for the Analysis of Soil Liquefaction Problems, Davis, California, 1993, 67-86.

[19] Arias, A., A Measure of Earthquake Intensity, Seismic Design for Nuclear Power Plants, R. J. Hansen, ed., MIT Press, Cambridge, Mass, 1970.

[20] Dashti, S., Bray, J.D., Pestana, J.M., Riemer, M., and Wilson, D., Centrifuge Testing to Evaluate and Mitigate Liquefaction-Induced Building Settlement Mechanisms, ASCE, Journal of

Geotechnical and Geoenvironmental Engineering, 136(7), 2010, 918-929.

[21] Ketchum, S.A., Ko, H.-Y., and Sture, S., Performance of an Earthquake Motion Simulator for a Small Geotechnical Centrifuge, Centrifuge 91, Ko (ed.), Balkema, Rotterdam, 1991, 361-368.

[22] Idriss, I.M. and Seed, H.B., Seismic Performance of Horizontal Soil Layers, ASCE, Journal of Soil Mechanics and Foundations Division, 1968, 94 (SM4), 1003-1031.

[23] Seed H.B. and Idriss I.M., Soil moduli and damping factors for dynamic response analyses, Rep. No. EERC 70-10. Earthquake Engrg. Res. Ctr., Univ. of California, Berkeley, Calif., 1970.

[24] Hardin, B.O. and Richart, F.E., Elastic Wave Velocities in Granular Soils, ASCE, Journal of Soil Mechanics and Foundations Division, Proc., 98 (SM1), 33-68.

[25] Elgamal, A., Yang, Z., Lai, T., Kutter, B.L., and Wilson, D.W., Dynamic Response of Saturated Dense Sand in Laminated Centrifuge Container, ASCE, Journal of Geotechnical and Geoenvironmental Engineering, 131(5), 598-609.

[26] Darendeli, M.B. and Stokoe K.H., Development of a new family of normalized modulus reduction and material damping curves, University of Texas, Geotechnical Engineering Report GD01-1, 2001.

[27] Chiu, P., Pradel, D.E., Kwok, A. O.-L., and Stewart, J.P., Seismic Response Analyses for the Silicon Valley Rapid Transit Project, Geotechnical Earthquake Engineering and Soil Dynamics IV (GSP 181), Sacramento, CA, 2008.

[28] Hashash, Y.M.A., Phillips, C., Groholski, D.R., Recent Advances in Nonlinear Site Response Analysis, 5th International Conference on Recent Advances in Geotechnical Earthquake Engineering and Soil Dynamics, San Diego, California, May 24-29, 2010, 1-22.

List of Table and Figure Captions

Table 1: Container material properties used in the numerical simulations with ABAQUS

Material	Density (kg/m³)	Elastic Modulus (MPa)	Poisson's Ratio	Material Model
Aluminum	2,713	68,900	0.33	Elastic
Clear Acrylic	1,010	2,930	0.3	Elastic
Neoprene Rubber	960	2~4*	0.49	Viscoelastic

* Pressure dependent material where a pressure range of 50 to 200 kPa

Table 2: Centrifuge test plan

TEST Name	Centrifuge g-level	Test Type	Tested Motion
FF-AMB55	55	Free Field	Ambient
FF-IZM60	60	Free Field	Izmit
FF-LND77	77	Free Field	Landers
SSI-LND77	77	SSI	Landers

Table 3: Physical properties of Nevada sand

Specific Gravity	2.65
Maximum Dry Unit Weight	16.4 kN/m³
Minimum Void Ratio	0.59
Minimum Dry Unit Weight	14 kN/m³
Maximum Void Ratio	0.85
c_u *	1.67 kPa
ϕ, Friction Angle *	33°

* Reference [17]

Table 4: Characteristics of the selected input earthquake ground motion (at original scale) for dynamic characterization of the FSB container

EQ. Motion	Year	Station	Magnitude	PGA (g)	Dominant Period T_P (sec)	Arias Intensity (m/s)	Significant Duration D5-95 (sec)	Shaking Intensity Rate (m/s²)	Distance to Rupture (km)
Izmit	1999	Istanbul	7.5	0.05	0.22	0.4	38.1	0.014	52
Landers	1992	Joshua Tree	7.3	0.3	0.72	2.4	26.1	0.075	11
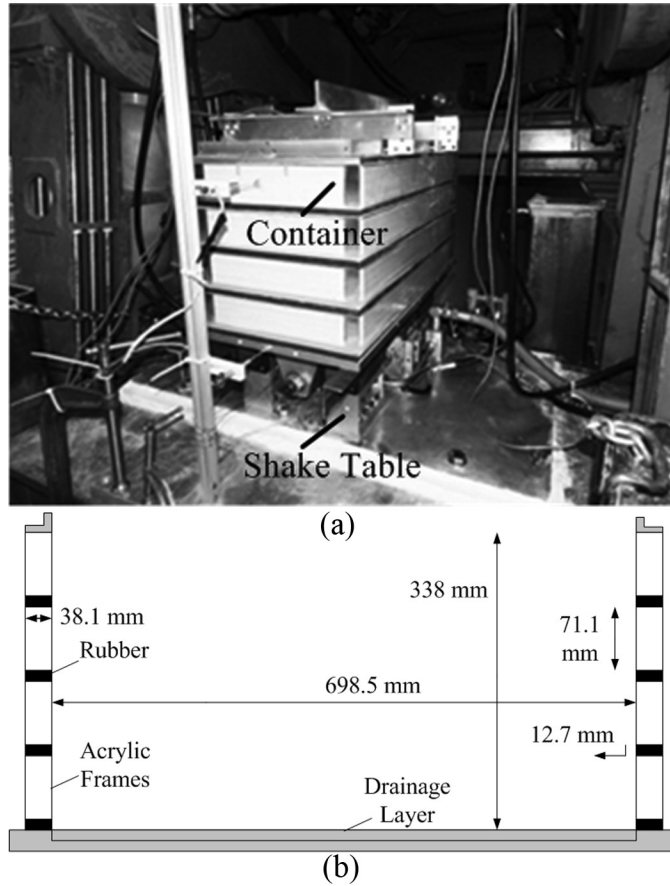
Figure 1: The transparent FSB container at CU Boulder: (a) photograph showing the FSB container placed on the shaker mounted on the centrifuge platform; (b) the schematic drawing of the container.
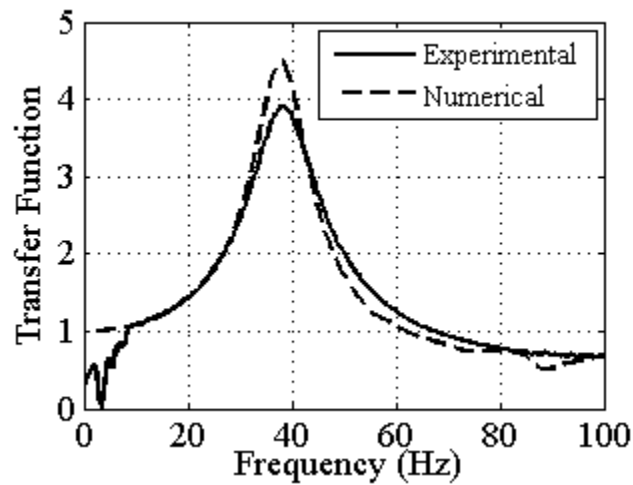
Figure 2: Frequency response transfer functions of the empty container at 60 g of centrifuge acceleration obtained numerically and experimentally.
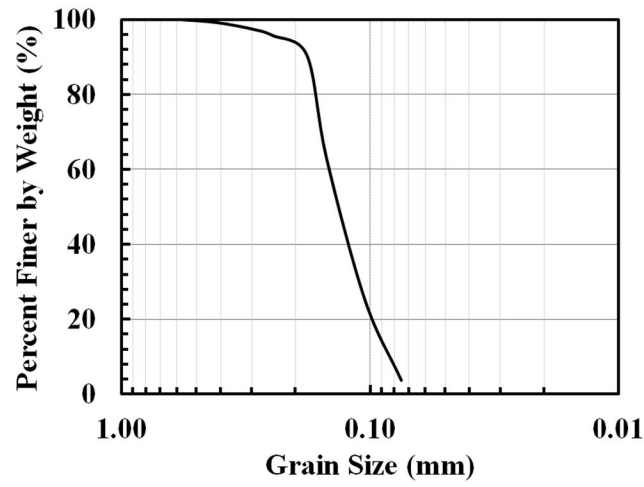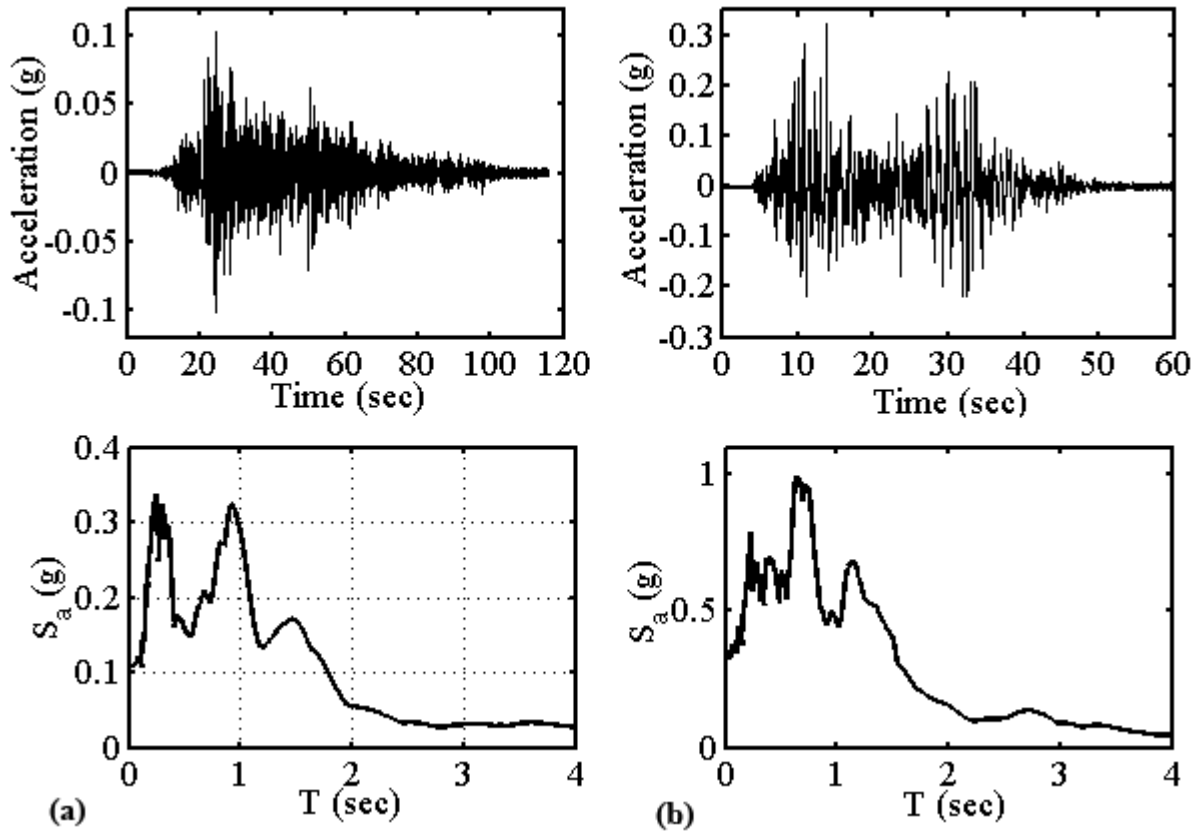
Figure 3: Grain size distribution for Nevada sand.

(a)

(b)

Figure 4: Acceleration-time histories and 5%-damped spectral accelerations of the: (a) Izmit motion; (b) Landers motion.
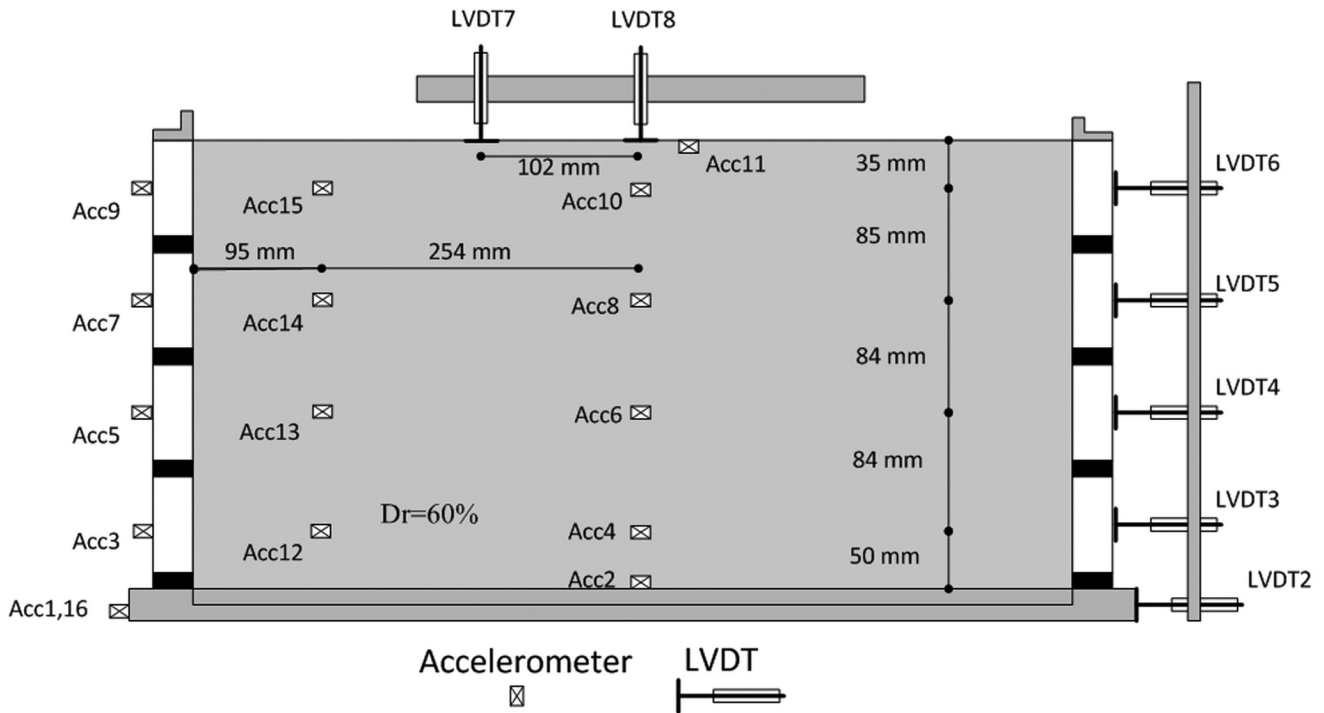
Figure 5: Schematics of the instrumentation layout for FF-AMB55, FF-IZM60, and FF-LND77 tests.
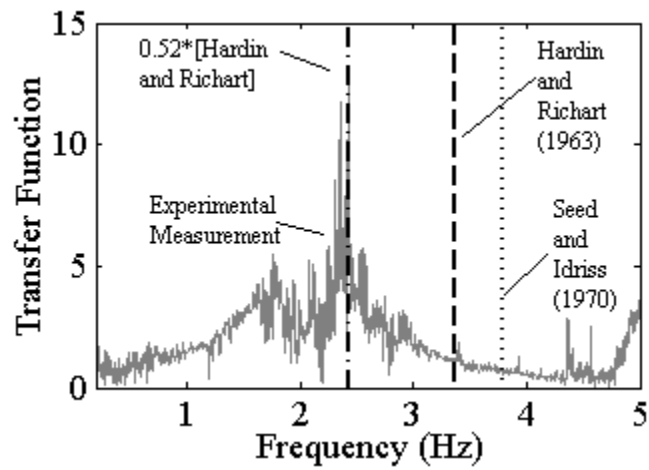
Figure 6: Frequency response transfer function of surface-to-base motion during the test FF-AMB55.
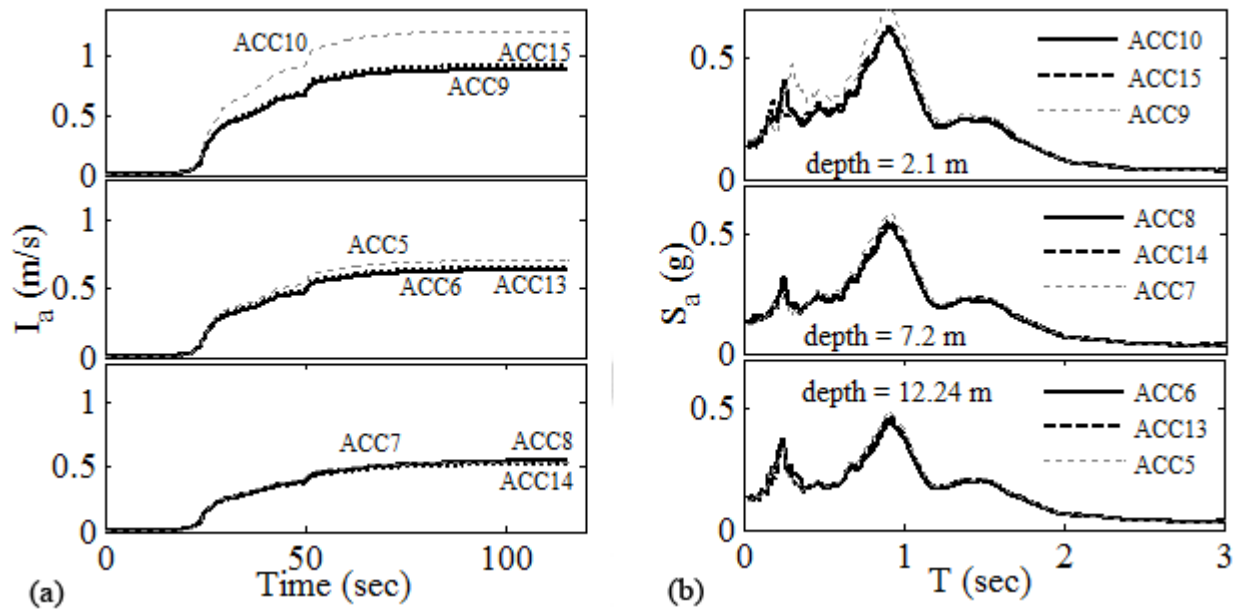
Figure 7: Comparison of the recorded motions at different depths across the container during the test FF-IZM60 in terms of: (a) Arias Intensity-time histories (I_a); and (b) 5%-damped spectral accelerations (S_a).
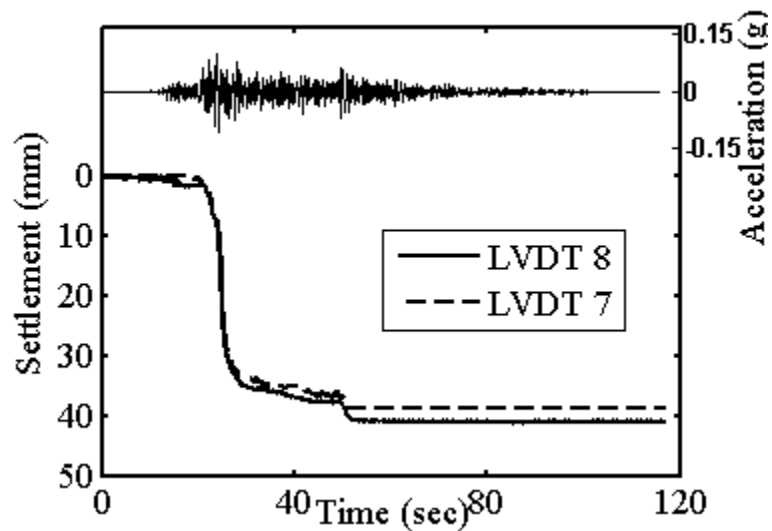
Figure 8: Center and off-center prototype surface settlement comparisons during the test FF-IZM60.
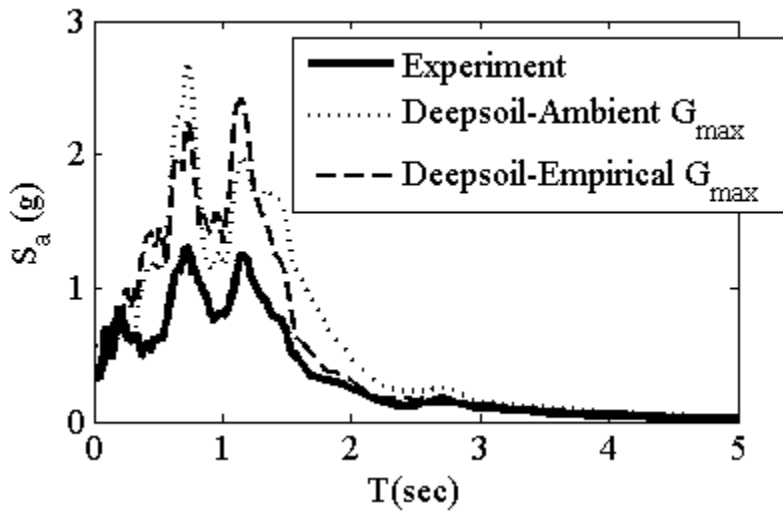
Figure 9: Comparison of 5%-damped spectral accelerations measured at the soil surface in test FF-LND77 with the corresponding 1-D, equivalent-linear site response analyses using DEEPSOIL.
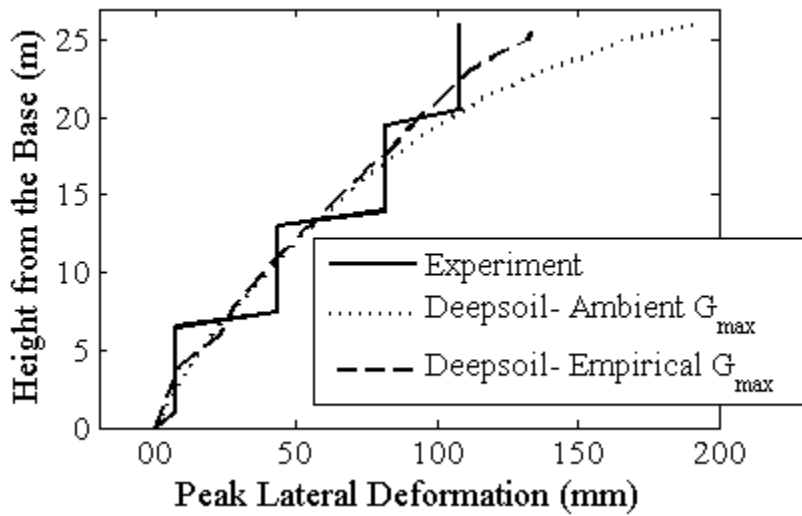
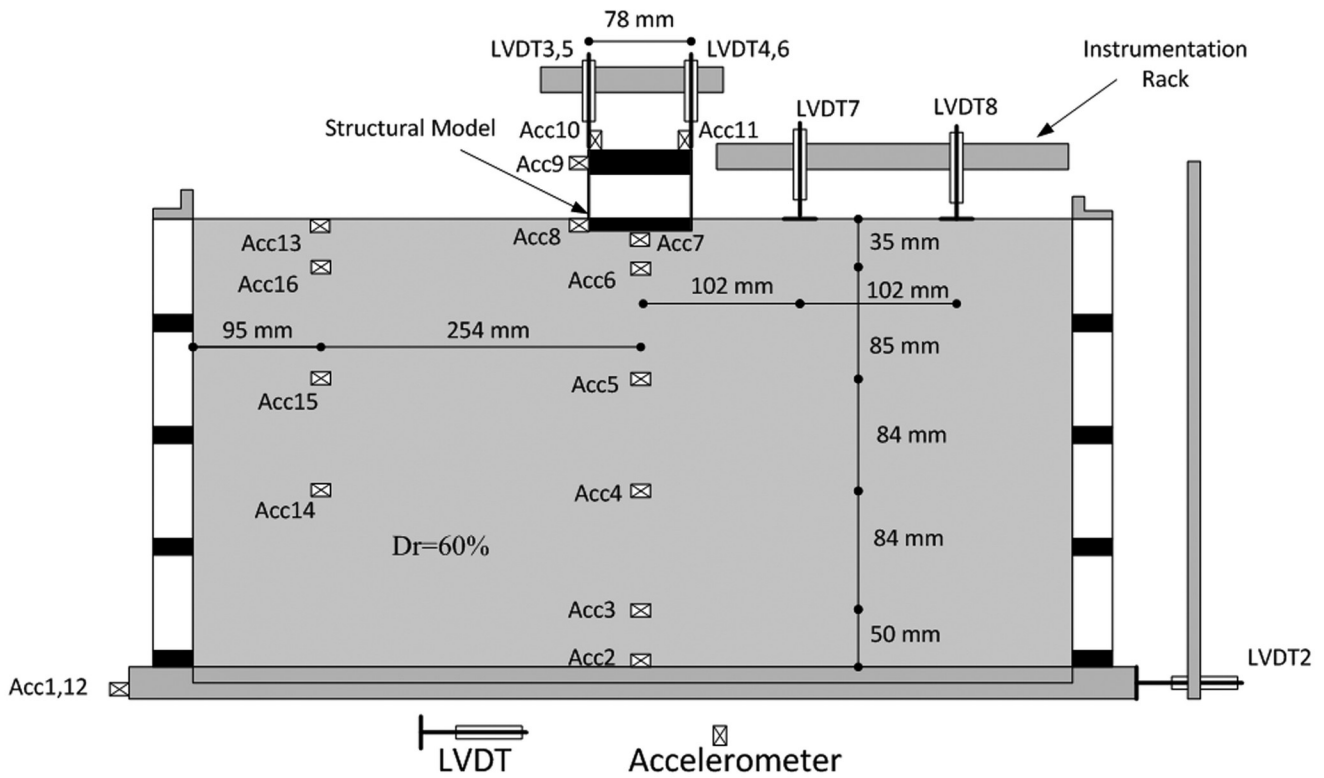Figure 10: Maximum lateral deformation profiles: Experiment vs. DEEPSOIL.

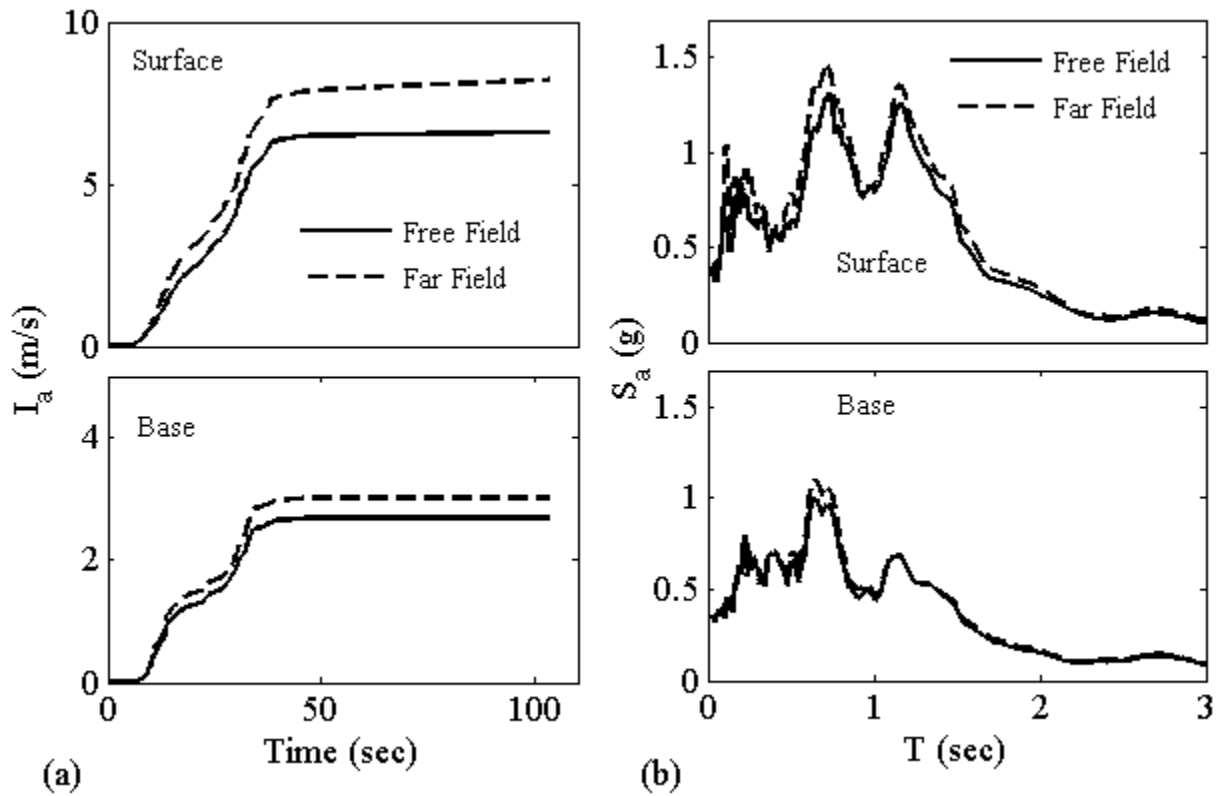Figure 11: Schematics of the instrumentation layout for experiment SSI-LND77.

Figure 12: Comparison of base and surface accelerations in the free-field (test FF-LND77) with far-field (test SSI-LND77) in terms of: (a) Arias Intensity (I_a); (b) 5%-damped Spectral Acceleration (S_a).
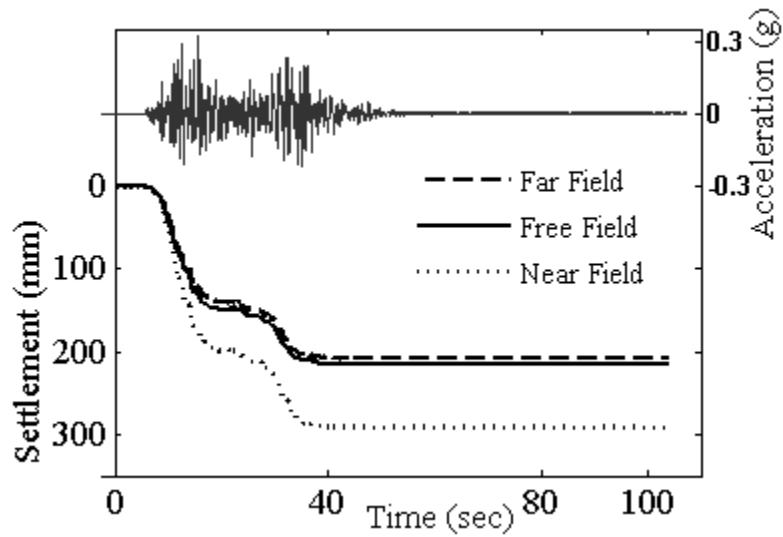
Figure 13: Comparison of settlements in the free-field, far-field, and near-field in Tests FF-LND77 and SSI-LND77.
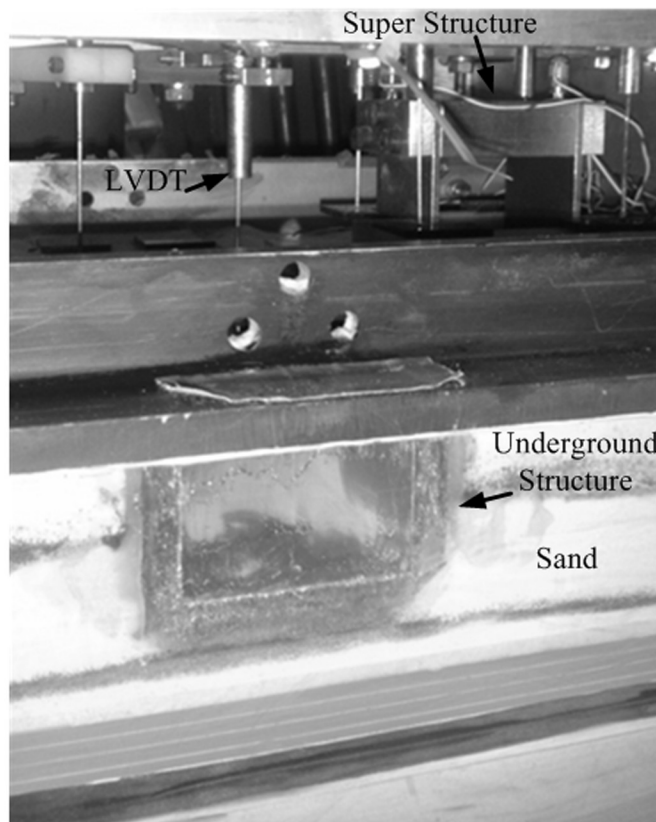

Figure 14: Photograph of an underground structure adjacent to a building model placed in the transparent FSB container which is mounted on the centrifuge shake table during a test to investigate soil-structure interaction for an underground structure.